All-Wheel Steering Vehicle Control Based on Contraction Theory with Neural Network

1st Myeongseok Ryu and 2nd Kyunghwan Choi
Cho Chun Shik Graduate School of Mobility
Korea Advanced Institute of Science and Technology (KAIST)
Daejeon, Republic of Korea
{dding_98, kh.choi}@kaist.ac.kr

***Abstract*—All-wheel steering (AWS) vehicles have been widely studied in the literature to enhance stability and maneuverability. In this study, we propose a contraction theory-based AWS vehicle control strategy integrated with neural networks (NNs). Contraction theory is a powerful tool for designing controllers for nonlinear systems, ensuring the incremental exponential convergence of all system trajectories to a unique trajectory, regardless of initial conditions. However, control performance may degrade due to system uncertainties. To address this issue, NNs are employed to approximate and compensate for these system uncertainties. The contraction property is guaranteed by formulating Linear Matrix Inequalities (LMIs) to obtain the contraction metric. Furthermore, the adaptation law for the NN weights is designed using Lyapunov theory to ensure the stability of the closed-loop system. Finally, numerical simulation results are provided to validate the proposed control strategy.**

***Index Terms*—All-wheel steering, Contraction theory, Neural networks**

NOTATION

In this study, the following notation is used: Vector and matrix entries are denoted as $\boldsymbol{x} = [x_i]_{i\in\{1,\cdots,n\}}$ and $\boldsymbol{A} = [a_{ij}]_{i\in\{1,\cdots,n\},j\in\{1,\cdots,m\}}$, respectively. The symmetric part of a matrix is denoted as $\mathrm{sym}(\boldsymbol{A}) := \frac{1}{2}(\boldsymbol{A} + \boldsymbol{A}^\top)$ [1]. The Kronecker product is denoted by $\otimes$ [2, Chap. 7 Def. 7.1.2]. The identity matrix of size n is denoted by $\boldsymbol{I}_n$, and the zero matrix of size $n \times m$ is denoted by $\boldsymbol{0}_{n\times m}$. The i^{th} row of the matrix $\boldsymbol{A} \in \mathbb{R}^{n\times m}$ is denoted by $\mathrm{row}_i(\boldsymbol{A})$. For $\boldsymbol{A} \in \mathbb{R}^{n\times m}$, the vectorization of $\boldsymbol{A}$ is denoted as $\mathrm{vec}(\boldsymbol{A}) := (\mathrm{row}_1(\boldsymbol{A}^\top), \cdots, \mathrm{row}_m(\boldsymbol{A}^\top))^\top \in \mathbb{R}^{nm}$.

I. INTRODUCTION

A. Motivation

Over the past decade, various control strategies have been investigated to improve the safety and control performance of vehicle systems. In particular, as all-wheel steering (AWS) vehicles have gained popularity due to their superior maneuverability and stability compared to front-wheel steering (FWS) vehicles [3], the motion control of AWS vehicles has been actively studied [4]–[7]. Conventionally, proportional control based on the front steering angle has been widely used for the rear steering angle of AWS vehicles due to its simplicity and ease of implementation. However, this method has limitations in achieving optimal control performance due to the phase difference between the side slip angle and the yaw rate of the vehicle [8], i.e., the transient response performance may degrade. Consequently, more advanced control strategies have been proposed to improve the transient response, such as Model Predictive Control (MPC) [5], Sliding Mode Control (SMC) [6], and robust control [7].

In recent years, contraction theory has been proposed as an alternative nonlinear control design method [1], [9]. Unlike traditional Lyapunov theory, which focuses on the stability of a system with respect to an equilibrium point, contraction theory analyzes the differential dynamics of the system to ensure the convergence between system trajectories [9]. Significantly, leveraging the differential nature of contraction theory, several studies have proposed the Linear Time-Varying (LTV) system type design method [10]–[12]. These approaches provide simpler and more systematic design procedures by formulating Linear Matrix Inequalities (LMIs) to obtain the contraction metric, which is then used as a feedback gain in the controller design [10].

In practice, however, contraction theory-based controller performance may be compromised by various uncertainties in the system models, since the contraction metric is derived based on the nominal system model. Specifically, for vehicle systems, tire cornering stiffness is a highly uncertain parameter that varies with state and road conditions [13]. Some studies have introduced adaptive control strategies to handle such uncertainties [11], [14]. Nevertheless, these methods require the exact model structure of the uncertainties, which is difficult to obtain in practical scenarios.

To address this, neural networks (NNs) have been incorporated into adaptive control frameworks to approximate unknown system functions, including uncertainties [15]–[17]. The primary advantage of NNs is their ability to approximate any sufficiently smooth function with arbitrary accuracy, provided there are enough neurons [18]. Thus, unknown functions can be modeled using user-designed NN structures with ideal weights and bounded approximation errors, allowing traditional adaptive control techniques to be applied in designing online adaptation laws [17] ensuring the system stability.

In this context, NNs can be utilized to approximate and compensate for uncertain functions in vehicle systems, thereby

This work was supported in part by the National Research Foundation of Korea (NRF) grant funded by the Korea government (MSIT) (RS-2025-00554087)

enhancing the performance of contraction theory-based controllers. To the best of our knowledge, no previous work has combined NNs with a contraction theory-based control strategy to handle uncertainties in vehicle systems online. Therefore, the main objective of this paper is to extend the contraction theory-based vehicle control strategy to account for system uncertainties.

B. Contributions

The main contributions of this study are as follows:

- A contraction metric is derived using Linear Matrix Inequalities (LMIs), which simplifies the calculation, and the uncertainties in the control input matrix are considered, assuming the worst-case scenario;
- NNs are employed to approximate model uncertainties online to improve control performance; and
- The stability and steady-state error of the system are analyzed using Lyapunov theory.

C. Organization

The remainder of this paper is organized as follows. Section II presents the problem formulation and control objectives. Section III provides the necessary background on contraction theory. Section IV discusses the main results, including the proposed method. Section V presents the numerical validation. Finally, Section VI concludes the paper.

II. Problem Formulation and Control Objectives

In this study, the AWS vehicle is modeled as a simplified 2-DOF bicycle model. The following 2-DOF vehicle lateral dynamics are considered:

$$\begin{cases} mv_x(\frac{\mathrm{d}}{\mathrm{d}t}\beta + r) = F_f + F_r, \\ I_z \frac{\mathrm{d}}{\mathrm{d}t} r = F_f l_f - F_r l_r, \end{cases} \tag{1}$$

where m denotes the mass of the vehicle, I_z denotes the yaw moment of inertia, v_x denotes the constant longitudinal velocity, β denotes the side slip angle, r denotes the yaw rate, and l_f and l_r denote the distances from the center of gravity (CG) to the front and rear axles, respectively. The lateral forces at the front and rear tires are given by

$$F_f := C_f \underbrace{\left(\delta_f - (\beta + \tfrac{l_f r}{v_x})\right)}_{=:\alpha_f} \text{ and } F_r := C_r \underbrace{\left(\delta_r - (\beta - \tfrac{l_r r}{v_x})\right)}_{=:\alpha_r}, \tag{2}$$

where δ_f, δ_r and α_f, α_r denote the front/rear steering angle inputs and slip angles, respectively. The tire cornering stiffnesses C_f and C_r are uncertain parameters that vary with state and road conditions. From a practical standpoint, the cornering stiffnesses are assumed to be bounded such that $C_i \in [\underline{C}_i, \overline{C}_i]$ for known constants $\underline{C}_i, \overline{C}_i \in \mathbb{R}_{>0},\ \forall i \in \{f, r\}$. Furthermore, the actual lateral tire forces differ from the linear tire model (2), as tire forces are highly nonlinear functions that include saturation behaviors [13, Chap. 13].

Using contraction theory, we can design a feedback controller that renders the vehicle system (1) contracting to a desired trajectory, i.e., the system trajectories exponentially converge to the desired trajectory regardless of initial conditions. However, owing to the uncertainties in the cornering stiffnesses and potential disturbances, the feedback controller's performance may degrade. To tackle these issues, the control objectives of this study are twofold:

- Design a feedback controller that makes the vehicle system contract to the desired trajectories, considering the worst-case scenario of the uncertainties; and
- Approximate the uncertainties from the cornering stiffnesses online by using NNs to improve the performance.

III. Preliminaries

In this section, we provide the necessary background on contraction theory. The detailed explanation of contraction theory can be found in [9], [19].

Consider that we have the following deterministic nonlinear system:

$$\tfrac{\mathrm{d}}{\mathrm{d}t}\boldsymbol{x} = \boldsymbol{f}(\boldsymbol{x}, t), \tag{3}$$

where $\boldsymbol{x} \in \mathbb{R}^n$ denotes the state vector and $\boldsymbol{f} : \mathbb{R}^n \times \mathbb{R}_{\geq 0} \to \mathbb{R}^n$ denotes a smooth nonlinear vector function. Contraction theory commences with the definition of the differential dynamics of the system (3) using differential displacement $\delta\boldsymbol{x}$ [20, Chap 4], which is defined as follows:

$$\tfrac{\mathrm{d}}{\mathrm{d}t}\delta\boldsymbol{x} = \tfrac{\partial \boldsymbol{f}}{\partial \boldsymbol{x}}\delta\boldsymbol{x}. \tag{4}$$

The contraction property of the system (3) can be analyzed using the Lyapunov function $V_c := V_c(\boldsymbol{x}, t) = \frac{1}{2}\delta\boldsymbol{x}^\top \boldsymbol{M}\delta\boldsymbol{x}$, where $\boldsymbol{M} := \boldsymbol{M}(\boldsymbol{x}, \boldsymbol{x}_d, t) \in \mathbb{R}^{n\times n}$ denotes the contraction metric. The contraction metric $\boldsymbol{M}$ is a symmetric positive definite matrix and satisfies $\overline{m}\boldsymbol{I}_n \succeq \boldsymbol{M} \succeq \underline{m}\boldsymbol{I}_n$ with $\overline{m}, \underline{m} \in \mathbb{R}_{>0}$. For the system (3) to be contracting, the following condition must hold:

$$\tfrac{\mathrm{d}}{\mathrm{d}t}\boldsymbol{M} + 2\,\mathrm{sym}(\boldsymbol{M}\tfrac{\partial \boldsymbol{f}}{\partial \boldsymbol{x}}) \leq -2\alpha\boldsymbol{M}, \tag{5}$$

which leads to $\frac{\mathrm{d}}{\mathrm{d}t}V_c \leq -\alpha V_c$ for some $\alpha \in \mathbb{R}_{>0}$. In other words, all solutions of the system (3) are contracting to a unique solution with an exponential rate α, i.e., the system is incrementally exponentially stable [9]. It is notable that the initial conditions are exponentially forgotten in the contracting system.

If the system (3) is perturbed by a bounded disturbance $\boldsymbol{d} := \boldsymbol{d}(\boldsymbol{x}, t) \in \mathbb{R}^n$ such that $\|\boldsymbol{d}\| \leq \overline{d}$, (3) can be rewritten as

$$\tfrac{\mathrm{d}}{\mathrm{d}t}\boldsymbol{x} = \boldsymbol{f}(\boldsymbol{x}, t) + \boldsymbol{d}. \tag{6}$$

The disturbance $\boldsymbol{d}$ can consist of various uncertainties such as parameter variations, unmodeled dynamics and external disturbances. According to the following theorem, a bounded error ball of the solutions of (3) and (6) is guaranteed to converge incrementally and exponentially.

Theorem 1 (Theorem 2.4 in [19] and Eq. (15) [9])**.** *If the system* (3) *is contracting with the contraction metric* $\boldsymbol{M}$ *which satisfies the condition* (5)*, the path integral* $V_l(\boldsymbol{q}, \delta\boldsymbol{q}, t) = \int_{\boldsymbol{\xi}_1}^{\boldsymbol{\xi}_2} \|\boldsymbol{\Theta}(\boldsymbol{q}, t)\delta\boldsymbol{q}\|$*, where* $\boldsymbol{\Theta}(\boldsymbol{q}, t) := \boldsymbol{M}^{1/2}$*, and* $\boldsymbol{\xi}_1$ *and* $\boldsymbol{\xi}_2$ *are the solutions of* (3) *and* (6)*, respectively, and* $\boldsymbol{q}$ *is the*

virtual state variable, exponentially converges to a bounded ball. Especially, the following inequality of a bounded error ball of the solutions of (3) *and* (6) *holds:*

$$\|\boldsymbol{\xi}_1(t)-\boldsymbol{\xi}_2(t)\| \leq \frac{V_l(0)}{\sqrt{\underline{m}}}\exp(-\alpha t)+\frac{\bar{d}}{\alpha}\sqrt{\chi}(1-\exp(-\alpha t)), \tag{7}$$

where $\chi := \overline{m}/\underline{m}$ *denotes the condition number of* $\boldsymbol{M}$*, yielding the steady state error bound of* $\frac{\bar{d}}{\alpha}\chi$*.*

Proof. See the proof of Theorem 2.4 in [19]. □

IV. Main Results

We first design the feedback controller based on contraction theory, considering the worst-case scenario of uncertainties in Section IV-A. The feedback controller design is highly motivated by [19] which formulates an LMI optimization problem to find the contraction metric in the feedback controller. Then, the NN will be employed to approximate the lumped disturbance in the error dynamics and design the adaptation law to update the NN weights online ensuring the system's stability in Section IV-B.

A. Feedback Controller Using Contraction Theory

Consider the following nonlinear affine system:

$$\tfrac{\mathrm{d}}{\mathrm{d}t}\boldsymbol{x} = \boldsymbol{f}(\boldsymbol{x},\boldsymbol{\pi})+\boldsymbol{g}(\boldsymbol{x},\boldsymbol{\pi})\boldsymbol{u}+\boldsymbol{d}, \tag{8}$$

where $\boldsymbol{x}\in\Omega_x\subset\mathbb{R}^n$, $\boldsymbol{u}\in\mathbb{R}^m$, $\boldsymbol{\pi}\in\Omega_\pi\subset\mathbb{R}^p$, and $\boldsymbol{d}\in\mathbb{R}^n$ denote the state vector, control input, uncertain parameters, and additional bounded lumped disturbance vector, respectively, and Ω_x,Ω_π denote the feasible state and parameter domains, respectively. By denoting $\boldsymbol{x} := (\beta, r)^\top \in \mathbb{R}^2$, $\boldsymbol{u} := (\delta_f,\delta_r)^\top\in\mathbb{R}$ and $\boldsymbol{\pi} := (C_f, C_r)^\top\in\mathbb{R}^2$, the vehicle dynamics (1) with (2) can be rewritten as (8).

The system (8) is assumed to satisfy the following.

Assumption 1. *The uncertain parameters* $\boldsymbol{\pi}$ *are bounded as* $\pi_i\in[\underline{\pi}_i,\overline{\pi}_i]$ *for known positive constants* $\underline{\pi}_i,\overline{\pi}_i\in\mathbb{R}_{>0}$*.*

Assumption 2. *The system functions* $\boldsymbol{f}$ *and* $\boldsymbol{g}$ *are sufficiently smooth and Lipschitz continuous with some positive constants* $L_f, L_g\in\mathbb{R}_{>0}$*, and* $\boldsymbol{g}$ *is full column rank to guarantee the existence of* $\boldsymbol{g}^\dagger$*. Furthermore, the sign and upper/lower bounds of entries of* $\boldsymbol{g}$ *are known, for instance* $g_{ij}\in[\underline{g}_{ij},\overline{g}_{ij}]$ *for known positive constants* $\underline{g}_{ij},\overline{g}_{ij}\in\mathbb{R}_{>0}$*. Therefore, the upper/lower bounds of* $\|\boldsymbol{g}\|$ *are also known as* $\|\boldsymbol{g}\|\in[\underline{g},\overline{g}]$ *for known positive constants* $\underline{g},\overline{g}\in\mathbb{R}_{>0}$*.*

The desired trajectory $\boldsymbol{x}_d := \boldsymbol{x}_d(t)\in\Omega_x\subset\mathbb{R}^n$ is assumed to be given by simulating a pre-designed desired control input $\boldsymbol{u}_d := \boldsymbol{u}_d\in\mathbb{R}^m$ with nominal parameters $\boldsymbol{\pi}_n\in\Omega_\pi\subset\mathbb{R}^p$ as

$$\tfrac{\mathrm{d}}{\mathrm{d}t}\boldsymbol{x}_d = \boldsymbol{f}(\boldsymbol{x}_d,\boldsymbol{\pi}_n)+\boldsymbol{g}(\boldsymbol{x}_d,\boldsymbol{\pi}_n)\boldsymbol{u}_d. \tag{9}$$

Before designing the feedback controller, we derive the error dynamics of $\boldsymbol{e} := \boldsymbol{x}-\boldsymbol{x}_d\in\mathbb{R}^n$ as follows:

$$\tfrac{\mathrm{d}}{\mathrm{d}t}\boldsymbol{e} = \boldsymbol{f}(\boldsymbol{x},\boldsymbol{\pi})-\boldsymbol{f}(\boldsymbol{x}_d,\boldsymbol{\pi}_n)+\boldsymbol{g}(\boldsymbol{x},\boldsymbol{\pi})\boldsymbol{u}-\boldsymbol{g}(\boldsymbol{x}_d,\boldsymbol{\pi}_n)\boldsymbol{u}_d+\boldsymbol{d}. \tag{10}$$

Invoking the state-dependent coefficient (SDC) formulation which is defined as $\mathbb{A} := \mathbb{A}(\boldsymbol{x},\boldsymbol{x}_d) = \int_0^1\left[\frac{\partial\overline{\boldsymbol{f}}}{\partial\boldsymbol{x}}\right](c\boldsymbol{x}+(1-c)\boldsymbol{x}_d)\,\mathrm{d}c$, where $\overline{\boldsymbol{f}} := \boldsymbol{f}(\boldsymbol{x},\boldsymbol{\pi}_n)-\boldsymbol{f}(\boldsymbol{x}_d,\boldsymbol{\pi}_n)+(\boldsymbol{g}(\boldsymbol{x},\boldsymbol{\pi}_n)-\boldsymbol{g}(\boldsymbol{x}_d,\boldsymbol{\pi}_n))\,\boldsymbol{u}_d$, i.e., see [12, Lemma 1], the error dynamics (10) can be represented in the LTV form as follows:

$$\tfrac{\mathrm{d}}{\mathrm{d}t}\boldsymbol{e} = \mathbb{A}(\boldsymbol{x}-\boldsymbol{x}_d)+\boldsymbol{g}(\boldsymbol{x},\boldsymbol{\pi})(\boldsymbol{u}-\boldsymbol{u}_d)+\boldsymbol{\delta}, \tag{11}$$

where $\overline{\boldsymbol{f}} = \mathbb{A}(\boldsymbol{x}-\boldsymbol{x}_d)$ and $\boldsymbol{\delta} := \boldsymbol{\delta}(\boldsymbol{x},\boldsymbol{\pi},\boldsymbol{\pi}_n,\boldsymbol{u}_d) = \boldsymbol{f}(\boldsymbol{x},\boldsymbol{\pi})-\boldsymbol{f}(\boldsymbol{x},\boldsymbol{\pi}_n)+(\boldsymbol{g}(\boldsymbol{x},\boldsymbol{\pi})-\boldsymbol{g}(\boldsymbol{x},\boldsymbol{\pi}_n))\boldsymbol{u}_d+\boldsymbol{d}$ denotes the lumped disturbance term which is bounded by Assumption 1 and 2.

The feedback control input $\boldsymbol{u}$ is designed as

$$\boldsymbol{u} := \boldsymbol{u}_d-\boldsymbol{R}^{-1}\boldsymbol{g}^\top(\boldsymbol{x},\boldsymbol{\pi}_n)\boldsymbol{M}\boldsymbol{e}+\boldsymbol{\nu}, \tag{12}$$

where $\boldsymbol{M}$ denotes the contraction metric to be obtained later, $\boldsymbol{R}\in\mathbb{R}^{m\times m}$ denotes a positive definite weighting matrix, and $\boldsymbol{\nu}\in\mathbb{R}^m$ denotes an auxiliary control input to be designed later to handle the uncertainties in Section IV-B. The control input yields the closed-loop error dynamics as

$$\tfrac{\mathrm{d}}{\mathrm{d}t}\boldsymbol{e} = \left(\mathbb{A}-\boldsymbol{g}\boldsymbol{R}^{-1}\boldsymbol{g}_n^\top\boldsymbol{M}\right)\boldsymbol{e}+\boldsymbol{g}\boldsymbol{\nu}+\boldsymbol{\delta}, \tag{13}$$

where $\boldsymbol{g} := \boldsymbol{g}(\boldsymbol{x},\boldsymbol{\pi})$ and $\boldsymbol{g}_n := \boldsymbol{g}(\boldsymbol{x},\boldsymbol{\pi}_n)$.

To apply Theorem 1, we define the systems (3) and (6) as (13) with $\boldsymbol{g}\boldsymbol{\nu}+\boldsymbol{\delta}=\boldsymbol{0}$ and (13), respectively, and the virtual $\boldsymbol{q}$-system as $\frac{\mathrm{d}}{\mathrm{d}t}(\boldsymbol{q}-\boldsymbol{x}_d) = (\mathbb{A}-\boldsymbol{g}\boldsymbol{R}^{-1}\boldsymbol{g}_n^\top\boldsymbol{M})(\boldsymbol{q}-\boldsymbol{x}_d)+\mu(\boldsymbol{g}\boldsymbol{\nu}+\boldsymbol{\delta})$, $\mu\in[0,1]$, whose solutions are denoted by $\boldsymbol{q}(\mu=0,t) =: \boldsymbol{\xi}_1$ and $\boldsymbol{q}(\mu=1,t) =: \boldsymbol{\xi}_2$, respectively. Then, by Theorem 1, the solutions $\boldsymbol{\xi}_1$ and $\boldsymbol{\xi}_2$ incrementally converge yielding the following steady state error bound:

$$\lim_{t\to\infty}\|\boldsymbol{e}(t)\| = \sup_{\boldsymbol{x}\in\Omega_x,\boldsymbol{\pi},\boldsymbol{\pi}_n\in\Omega_\pi}\|\boldsymbol{g}\boldsymbol{\nu}+\boldsymbol{\delta}\|\tfrac{\sqrt{\chi}}{\alpha}, \tag{14}$$

provided that the contraction metric $\boldsymbol{M}$ satisfies the following condition:

$$\tfrac{\mathrm{d}}{\mathrm{d}t}\boldsymbol{M}+2\,\mathrm{sym}(\boldsymbol{M}\mathbb{A})-2\,\mathrm{sym}(\boldsymbol{M}\boldsymbol{g}\boldsymbol{R}^{-1}\boldsymbol{g}_n^\top\boldsymbol{M})\preceq-2\alpha\boldsymbol{M}. \tag{15}$$

Note that $\|\boldsymbol{g}\boldsymbol{\nu}+\boldsymbol{\delta}\|$ can be considered as bounded disturbances in Theorem 1, since $\boldsymbol{g}$ and $\boldsymbol{\delta}$ are bounded and the boundedness of the auxiliary control input $\boldsymbol{\nu}$ will be shown in Section IV-B by designing the NN adaptation law.

Now, we formulate an LMI optimization problem to find the contraction metric $\boldsymbol{M}$ [19]. To transform Bilinear Matrix Inequality (BMI) condition (15) of $\boldsymbol{M}$, which corresponds to the contraction condition given in Theorem 1, into an LMI condition, $\boldsymbol{W} := \boldsymbol{M}^{-1}$ is pre- and post-multiplied to (15) as follows:

$$-\tfrac{\mathrm{d}}{\mathrm{d}t}\boldsymbol{W}+2\,\mathrm{sym}(\mathbb{A}\boldsymbol{W})+2\alpha\boldsymbol{W}\preceq 2\,\mathrm{sym}\left(\boldsymbol{g}\boldsymbol{R}^{-1}\boldsymbol{g}_n^\top\right), \tag{16}$$

leading to the LMI condition of $\boldsymbol{W}$. By Assumption 2, the right-hand side of (16) is positive symmetric definite. Thus, to satisfy (16) for all $g_{ij}\in[\underline{g}_{ij},\overline{g}_{ij}]$, the worst-case scenario is considered as $\underline{\boldsymbol{g}} = [\underline{g}_{ij}]_{i\in\{1,\cdots,n\},j\in\{1,\cdots,m\}}$, yielding the following LMI condition:

$$-\tfrac{\mathrm{d}}{\mathrm{d}t}\boldsymbol{W}+2\,\mathrm{sym}(\mathbb{A}\boldsymbol{W})+2\alpha\boldsymbol{W}\preceq 2\,\mathrm{sym}\left(\underline{\boldsymbol{g}}\boldsymbol{R}^{-1}\boldsymbol{g}_n^\top\right). \tag{17}$$

Finally, we obtain the LMI optimization problem to find $\boldsymbol{W} = \boldsymbol{M}^{-1}$ to satisfy the contraction condition (15) and

minimize the steady state error (14) by the condition number χ of $\boldsymbol{M}$, as follows:

$$\min_{\overline{\boldsymbol{W}},\chi,\mu} \chi + \lambda\mu$$

$$\text{s.t. } \begin{cases} \boldsymbol{I}_n \preceq \overline{\boldsymbol{W}} \preceq \chi \boldsymbol{I}_n \\ -\frac{\mathrm{d}}{\mathrm{d}t}\overline{\boldsymbol{W}} + 2\,\mathrm{sym}(\mathbb{A}\overline{\boldsymbol{W}}) + 2\alpha\overline{\boldsymbol{W}} \preceq 2\,\mathrm{sym}\left(\underline{\boldsymbol{g}}\boldsymbol{R}^{-1}\boldsymbol{g}_n^\top\right), \end{cases} \tag{18}$$

where $\mu := \overline{m}$ denotes an additional optimization variable representing the maximum limit of $\boldsymbol{M}$, $\overline{\boldsymbol{W}} := \overline{m}\boldsymbol{W}$ denotes the normalized $\boldsymbol{W}$ by μ, and $\lambda \in \mathbb{R}_{>0}$ denotes the penalty parameter of the maximum limit μ. By increasing λ, the amplitude of the control input can be decreased. The detailed and practical implementation of solving (18) can be found in [19], [21].

In conclusion, the feedback controller is designed to renders the system (8) contracting to the error bound exponentially with respect to the desired trajectory (9), by solving the LMI problem (18), considering the worst-case scenario of the uncertain input matrix.

B. Neural Network Approximation and Adaptation Law

In this section, NNs are employed to compensate for $\boldsymbol{\delta}$ in the error dynamics (13). The NNs $\boldsymbol{\Phi} : \mathbb{R}^{n+m} \times \mathbb{R}^{\Xi} \to \mathbb{R}^n$ approximate the desired auxiliary control input $\boldsymbol{\nu}^* := -\boldsymbol{g}^\dagger\boldsymbol{\delta}$ and the actual auxiliary control input $\boldsymbol{\nu}$ as follows:

$$\boldsymbol{\nu}^* = \boldsymbol{\Phi}(\boldsymbol{x}_n;\boldsymbol{\theta}^*) + \boldsymbol{\epsilon}, \text{ and } \boldsymbol{\nu} = \boldsymbol{\Phi}(\boldsymbol{x}_n;\widehat{\boldsymbol{\theta}}), \tag{19}$$

where $\boldsymbol{x}_n := (\boldsymbol{x}^\top, \boldsymbol{x}_d)^\top \in \mathbb{R}^{2n}$ denotes the NN input vector, $\boldsymbol{\theta}^* \in \mathbb{R}^{\Xi}$ and $\widehat{\boldsymbol{\theta}} \in \mathbb{R}^{\Xi}$ denote the vectorized ideal and estimated NN weights, respectively, and $\boldsymbol{\epsilon} \in \mathbb{R}^n$ denotes the bounded approximation error, such that $\|\boldsymbol{\epsilon}\| \le \overline{\epsilon} \in \mathbb{R}_{>0}$. The NN structure $\boldsymbol{\Phi}(\cdot)$ is defined as follows:

$$\boldsymbol{\Phi}(\boldsymbol{x}_n;\boldsymbol{\theta}) := \boldsymbol{W}_1^\top \boldsymbol{\phi}(\boldsymbol{W}_0^\top \boldsymbol{x}_n), \tag{20}$$

where $\boldsymbol{W}_0 \in \mathbb{R}^{2n+1\times l}$ and $\boldsymbol{W}_1 \in \mathbb{R}^{l+1\times m}$ denote weight matrices, and $\boldsymbol{\theta} := \left(\boldsymbol{\theta}_1^\top, \boldsymbol{\theta}_0^\top\right)^\top \in \mathbb{R}^{\Xi}$ denotes the vectorized NN weight vector argument with $\boldsymbol{\theta}_i := \mathrm{vec}(\boldsymbol{W}_i) \in \mathbb{R}^{\Xi_i},\ \forall i \in \{0,1\}$. The element-wise activation function $\boldsymbol{\phi}$ consists of $\tanh(\cdot)$ and 1 to incorporate a bias term in the weight matrix, i.e., $\boldsymbol{\phi}(\boldsymbol{z}) := (\tanh(z_1), \cdots, \tanh(z_l), 1)^\top \in \mathbb{R}^{l+1}$ for some $\boldsymbol{z} \in \mathbb{R}^l$. Hence, $\boldsymbol{\phi}$ is bounded and Lipschitz continuous, i.e., $\|\boldsymbol{\phi}(\cdot)\| \le \sqrt{l+1}$. The ideal NN weights $\boldsymbol{\theta}^*$ are assumed to be constant and bounded as $\|\boldsymbol{\theta}_i^*\| \le \overline{\theta}_i \in \mathbb{R}_{>0},\ \forall i \in \{0,1\}$.

The adaptation law of the NN weights is designed using Lyapunov stability theory. Consider the following Lyapunov candidate function of the error and outer NN weights estimation error $\tilde{\boldsymbol{\theta}}_1$: $V_1 := \frac{1}{2}\boldsymbol{e}^\top\boldsymbol{M}\boldsymbol{e} + \frac{1}{2}\tilde{\boldsymbol{\theta}}_1^\top\boldsymbol{\Gamma}_1^{-1}\tilde{\boldsymbol{\theta}}_1$, where $\boldsymbol{\Gamma}_1 \in \mathbb{R}^{\Xi_1\times\Xi_1}$ denotes the positive definite learning rate matrix. For brevity, we denote $\widehat{\boldsymbol{\phi}} := \boldsymbol{\phi}(\widehat{\boldsymbol{W}}_0\boldsymbol{x}_n)$ and $\boldsymbol{\phi}^* := \boldsymbol{\phi}(\boldsymbol{W}_0^*\boldsymbol{x}_n)$. By substituting the NNs in (19) into the closed-loop error dynamics (13), the time derivative of V_1 is given as

$$\begin{aligned}
\tfrac{\mathrm{d}}{\mathrm{d}t}V_1 \le\ & \underbrace{-\alpha\boldsymbol{e}^\top\boldsymbol{M}\boldsymbol{e}}_{\text{(15) is satisfied in (18)}} + \underbrace{\tilde{\boldsymbol{\theta}}_1^\top\boldsymbol{\Gamma}_1^{-1}\tfrac{\mathrm{d}}{\mathrm{d}t}\widehat{\boldsymbol{\theta}}_1}_{\because\ (\mathrm{d}/\mathrm{d}t)\boldsymbol{\theta}_1^*=0} \\
& + \boldsymbol{e}^\top\boldsymbol{M}\boldsymbol{g}\left(\boldsymbol{\Phi}(\boldsymbol{x}_n;\widehat{\boldsymbol{\theta}}) - \boldsymbol{\Phi}(\boldsymbol{x}_n;\boldsymbol{\theta}^*) - \boldsymbol{\epsilon}\right) \qquad (21) \\
\le & -\alpha\overline{m}\|\boldsymbol{e}\|^2 + \tilde{\boldsymbol{\theta}}_1^\top\boldsymbol{\Gamma}_1^{-1}\tfrac{\mathrm{d}}{\mathrm{d}t}\widehat{\boldsymbol{\theta}}_1 \\
& + \boldsymbol{e}^\top\boldsymbol{M}\boldsymbol{g}\left(\underbrace{(\boldsymbol{I}_{\Xi_1}\otimes\widehat{\boldsymbol{\phi}}^\top)\widehat{\boldsymbol{\theta}}_1 - (\boldsymbol{I}_{\Xi_1}\otimes\boldsymbol{\phi}^{*\top})\boldsymbol{\theta}_1^*}_{\text{see [2, Proposition (7.1.9)]}} - \boldsymbol{\epsilon}\right) \\
= & -\alpha\overline{m}\|\boldsymbol{e}\|^2 + \tilde{\boldsymbol{\theta}}_1^\top\boldsymbol{\Gamma}^{-1}\tfrac{\mathrm{d}}{\mathrm{d}t}\widehat{\boldsymbol{\theta}}_1 + \boldsymbol{e}^\top\boldsymbol{M}\boldsymbol{g}(\boldsymbol{I}_{\Xi_1}\otimes\widehat{\boldsymbol{\phi}}^\top)\tilde{\boldsymbol{\theta}}_1 \\
& + \underbrace{\boldsymbol{e}^\top\boldsymbol{M}\boldsymbol{g}^\top\left((\boldsymbol{I}_{\Xi_1}\otimes(\widehat{\boldsymbol{\phi}}-\boldsymbol{\phi}^*)^\top)\boldsymbol{\theta}_1^* - \boldsymbol{\epsilon}\right)}_{=:\boldsymbol{\Delta}_1},
\end{aligned}$$

where the last term $\boldsymbol{\Delta}_1 := \boldsymbol{\Delta}_1(\widehat{\boldsymbol{\theta}}_0, \boldsymbol{\theta}_0^*, \boldsymbol{\theta}_1^*)$ is bounded owing to the boundedness of the activation function, such that $\|\boldsymbol{\Delta}_1\| \le \overline{\delta_f}\|\boldsymbol{e}\|$ for a positive constant $\overline{\delta_f} := \overline{m}\,\overline{g}(2\sqrt{l+1}\,\overline{\theta}_1 + \overline{\epsilon}) \in \mathbb{R}_{>0}$.

To cancel out the third cross-coupling term on the right-hand side of the final equality in (21), the adaptation law $\frac{\mathrm{d}}{\mathrm{d}t}\widehat{\boldsymbol{\theta}}_1$ is designed as

$$\tfrac{\mathrm{d}}{\mathrm{d}t}\widehat{\boldsymbol{\theta}}_1 := -\boldsymbol{\Gamma}_1\Bigg(\underbrace{(\boldsymbol{I}_{\Xi_1}\otimes\widehat{\boldsymbol{\phi}})^\top}_{=(\partial\boldsymbol{\Phi}(\boldsymbol{x}_n;\widehat{\boldsymbol{\theta}})/\partial\widehat{\boldsymbol{\theta}}_1)^\top}\ \boldsymbol{g}_n^\top\boldsymbol{M}\boldsymbol{e} + \sigma_1\widehat{\boldsymbol{\theta}}_1\Bigg), \tag{22}$$

where the last term represents the σ-modification to ensure the boundedness of the NN weights [17, pp. 168-169] with a positive constant $\sigma_1 \in \mathbb{R}_{>0}$. Note that the nominal input matrix $\boldsymbol{g}_n$ is used instead of the actual input matrix $\boldsymbol{g}$, since the actual parameters $\boldsymbol{\pi}$ are unknown. Then, the time derivative of the Lyapunov candidate function (21) is given as

$$\begin{aligned}
\tfrac{\mathrm{d}}{\mathrm{d}t}V_1 \le & -\alpha\overline{m}\|\boldsymbol{e}\|^2 + \overline{\Delta}_1\|\boldsymbol{e}\| - \sigma_1\|\tilde{\boldsymbol{\theta}}_1\|^2 - \sigma_1\boldsymbol{\theta}^{*\top}_1\tilde{\boldsymbol{\theta}}_1 \\
& + \boldsymbol{e}^\top\boldsymbol{M}(\boldsymbol{g}-\boldsymbol{g}_n)\left(\boldsymbol{I}_{\Xi_1}\otimes\widehat{\boldsymbol{\phi}}^\top\right)\tilde{\boldsymbol{\theta}}_1 \\
\le & -\alpha\overline{m}\|\boldsymbol{e}\|^2 + \overline{\Delta}_1\|\boldsymbol{e}\| - \sigma_1\|\tilde{\boldsymbol{\theta}}_1\|^2 + \sigma_1\overline{\theta}_1\|\tilde{\boldsymbol{\theta}}_1\| \\
& + \underbrace{\overline{m}L_g\|\pi-\pi_n\|\|(\boldsymbol{I}_{\Xi_1}\otimes\widehat{\boldsymbol{\phi}}^\top)\|\|\boldsymbol{e}\|\|\tilde{\boldsymbol{\theta}}_1\|}_{\le\overline{m}L_g\overline{\pi}\sqrt{l+1}(\|e\|^2+\|\tilde{\boldsymbol{\theta}}_1\|^2),\ \text{(Young's inequality)}} \qquad (23) \\
\le & -\left(\alpha\overline{m} - \overline{m}L_g\overline{\pi}\sqrt{l+1}\right)\|\boldsymbol{e}\|^2 + \overline{\Delta}_1\|\boldsymbol{e}\| \\
& - \left(\sigma_1 - \overline{m}L_g\overline{\pi}\sqrt{l+1}\right)\|\tilde{\boldsymbol{\theta}}_1\|^2 + \sigma_1\overline{\theta}_1\|\tilde{\boldsymbol{\theta}}_1\|.
\end{aligned}$$

Hence, the error $\boldsymbol{e}$ and the NN weight estimation error $\tilde{\boldsymbol{\theta}}_1$ are uniformly ultimately bounded, if the parameters are chosen such that

$$\alpha > L_g\overline{\pi}\sqrt{l+1} \text{ and } \sigma_1 > \overline{m}L_g\overline{\pi}\sqrt{l+1}, \tag{24}$$

where the ultimate bounds are given as

$$\|e\| \le \tfrac{\overline{\Delta}_1}{\alpha\overline{m}-\overline{m}L_g\overline{\pi}\sqrt{l+1}}, \text{ and } \|\tilde{\boldsymbol{\theta}}_1\| \le \tfrac{\sigma_1\overline{\theta}_1}{\sigma_1-\overline{m}L_g\overline{\pi}\sqrt{l+1}}. \tag{25}$$

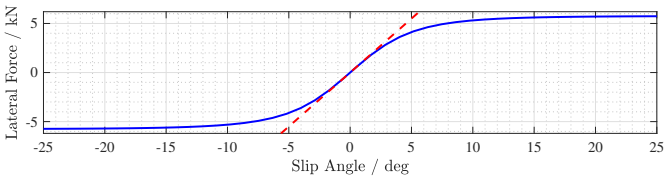

Fig. 1: Actual [—] and nominal [- - -] lateral tire models.

The adaptation law for the inner NN weights $\widehat{\boldsymbol{\theta}}_0$ can be designed in a similar manner as follows:

$$\frac{\mathrm{d}}{\mathrm{d}t}\widehat{\boldsymbol{\theta}}_0 := -\boldsymbol{\Gamma}_0\Bigg(\underbrace{\left(\widehat{\boldsymbol{W}}_1^\top(\boldsymbol{I}_{\Xi_0}\otimes\boldsymbol{x}_n^\top)\right)^\top}_{=(\partial\boldsymbol{\Phi}(\boldsymbol{x}_n;\widehat{\boldsymbol{\theta}})/\partial\widehat{\boldsymbol{\theta}}_0)^\top}\boldsymbol{g}_n^\top\boldsymbol{M}\boldsymbol{e}+\sigma_0\widehat{\boldsymbol{\theta}}_0\Bigg). \quad (26)$$

The boundedness of the inner NN weight estimation error $\tilde{\boldsymbol{\theta}}_0 := \widehat{\boldsymbol{\theta}}_0 - \boldsymbol{\theta}_0^*$ can be guaranteed and the corresponding conditions can be obtained similarly to the outer NN weights.

The boundedness of the auxiliary control input $\boldsymbol{\nu}$ in (12) can be guaranteed by the boundedness of the NN weights and the activation function.

V. Numerical Validation

A. Validation Setup

In this section, the proposed control method was validated in the vehicle lateral dynamics (1) with (2) via numerical simulation. The vehicle parameters were chosen as $m = 1463\,\mathrm{kg}$, $I_z = 1967.8\,\mathrm{kg\,m^2}$, $l_f = 1.2\,\mathrm{m}$, and $l_r = 1.6\,\mathrm{m}$. The nominal parameters were defined as $\boldsymbol{\pi}_n = (C_f, C_r)^\top = \left(6302\,\mathrm{N\,rad^{-1}}, 6302\,\mathrm{N\,rad^{-1}}\right)^\top$.

The actual lateral tire model was defined using the Magic Formula [13, pp. 365-366] which is defined as $F_{y_i} = D\sin\left[C\arctan\left\{B_i\alpha_i - E\left(B_i\alpha_i - \arctan(B_i\alpha_i)\right)\right\}\right]$, $\forall i \in \{f, r\}$, whose parameters were chosen as $C = 1.65$, $D = 5750$, and $E = 0.97$, and $B_f = 5.31$ and $B_r = 7.97$, as illustrated in Fig. 1. The slopes of the actual lateral front/rear tire models at $\alpha_i = 0$ were selected to be 80% and 120% of the nominal lateral tire stiffness for the front and rear tires, respectively, assuming that the vehicle is heavily loaded toward the rear. The disturbance vector $\boldsymbol{d}$ was chosen as a random signal sampled from a uniform distribution bounded by 10° and 20° for each state. Hence, the lumped disturbance term $\boldsymbol{\delta}$ in (11) included the parameter uncertainties in the lateral tire stiffness and the external disturbance $\boldsymbol{d}$.

The desired trajectory was generated by simulating with the nominal parameters $\boldsymbol{\pi}_n$ and the desired controller $\boldsymbol{u}_d$ which was simply chosen as a constant reverse-phase input of $\boldsymbol{u}_d(t) = (\delta_f, \delta_r)^\top = (3^\circ, -0.3^\circ)^\top$ at $t = 0.5\,\mathrm{s}$.

For comparative study, the conventional contraction theory-based controller [21] was also implemented. The selected controllers are summarized in Table I. The parameters for the feedback controllers were selected as $\alpha = 2$, $\boldsymbol{R} = \boldsymbol{I}_2$, and $\lambda = 5e{-}7$ and shared for both (C_1) and (C_2). The NN in (C_1) was designed with $l = 16$ hidden neurons and $\boldsymbol{\Gamma}_0 = \boldsymbol{\Gamma}_1 = 10\boldsymbol{I}_\Xi$, and $\sigma_0 = \sigma_1 = 0.001$. The upper/lower bounds for the lateral tire stiffness were chosen as $C_i \in [4141.4\,\mathrm{N\,rad^{-1}}, 8192.6\,\mathrm{N\,rad^{-1}}]$ for $i \in \{f, r\}$, considering $\pm 30\%$ variation from the nominal values.

The sampling rate for the controllers was set to $100\,\mathrm{Hz}$, while the simulation sampling rate was 10 times faster than the controllers.

TABLE I: Controllers for comparative study.

	Description	Control Input
(C_1) [—]	Proposed controller	(12)
(C_2) [—]	Conventional feedback controller based on contraction theory [21]	(12) without NN, i.e., $\boldsymbol{\nu} = \boldsymbol{0}$
(C_3) [—]	Desired controller	$\boldsymbol{u}_d$

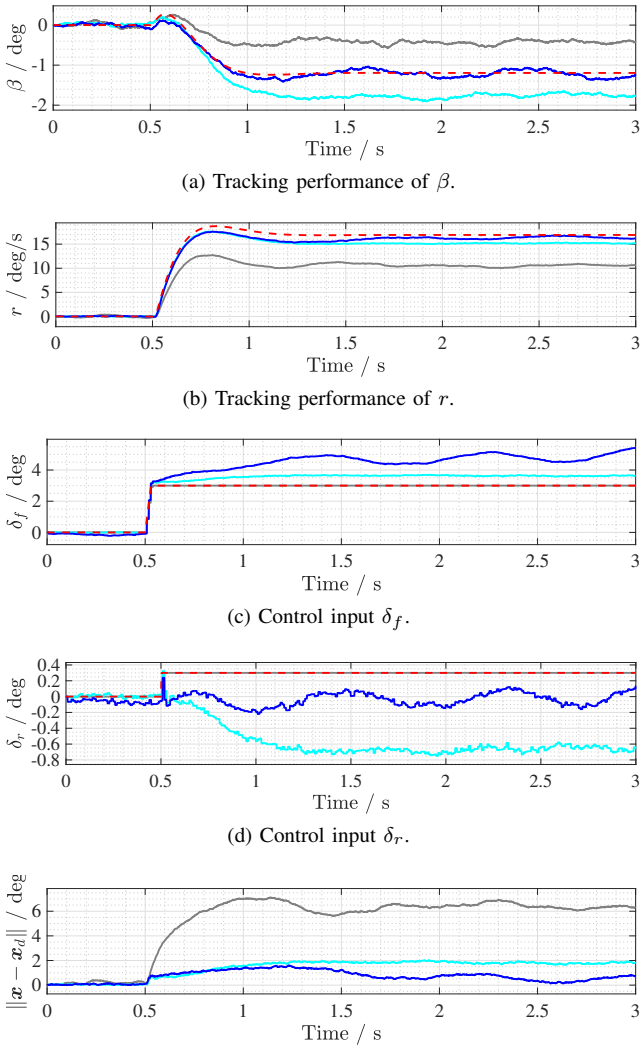

(a) Tracking performance of β.

(b) Tracking performance of r.

(c) Control input δ_f.

(d) Control input δ_r.

(e) Norm of tracking error $\|\boldsymbol{x} - \boldsymbol{x}_d\|$.

Fig. 2: Validation results of (C_1) [—], (C_2) [—] and (C_3) [—], and the desired trajectory [- - -].

B. Validation Results

The validation results are illustrated in Fig. 2. The tracking performances are quantitatively compared in Table II.

The simulated result of the desired system $\boldsymbol{x}_d$ with the nominal parameters $\boldsymbol{\pi}_n$ and the desired controller $\boldsymbol{u}_d$ is illustrated

TABLE II: Tracking performances in l_r norm.

	(C_1) [—]	(C_2) [—]	(C_3) [—]
$\int_0^T \|\boldsymbol{e}\| \, \mathrm{d}t$	0.0375 (-86.03%)	0.0727 (-72.95%)	0.2688 (–)

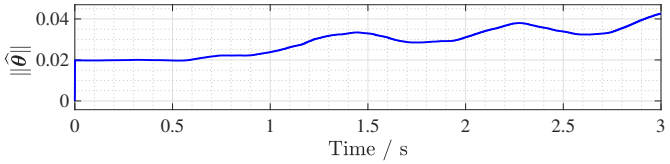

Fig. 3: Norm of neural network weights in (C_1).

in red dotted line in Fig. 2. Due to the model uncertainties and external disturbances, when the desired controller (C_3) was naively applied, the actual system $\boldsymbol{x}$ could not follow the desired trajectory $\boldsymbol{x}_d$, as illustrated in Fig. 2a and 2b, yielding large tracking errors 0.2688 as shown in Fig. 2e and Table II.

By applying the controllers based on contraction theory, i.e., (C_1) and (C_2), the trajectory errors between $\boldsymbol{x}$ and $\boldsymbol{x}_d$ were significantly reduced by 86.03% and 72.95% for (C_1) and (C_2), respectively, compared to (C_3), as summarized in Table II. In the case of (C_2), however, the tracking error was still observed, since the feedback controller was designed based on the worst-case scenario, as illustrated in Fig. 2e, yielding 94% higher tracking error than (C_1), as summarized in Table II.

In contrast, the proposed controller (C_1) employing NNs successfully compensated for the model uncertainties and external disturbances, yielding the best tracking performance among the tested controllers, as illustrated in Fig. 2e and Table II. The results demonstrated that the NNs effectively approximated and compensated for the residual model uncertainties and external disturbances, which could not be handled by the feedback controller designed based on the worst-case scenario (C_2). Moreover, during the online adaptation of the NN weights, the system including NN weights remained stable without any adverse effects, demonstrating the effectiveness of the proposed adaptation laws, as illustrated in Fig. 3.

VI. Conclusion

In this paper, we proposed an all-wheel steering vehicle lateral control method based on contraction theory with neural network adaptation to handle model uncertainties and external disturbances. The contraction theory-based feedback controller was designed to guarantee exponential convergence of the trajectory tracking error to a bounded region, considering the worst-case scenario of the model uncertainties. Then, NNs were employed to approximate and compensate for the residual model uncertainties and external disturbances, and the adaptation laws of the NN weights were designed to guarantee the boundedness of the tracking error and NN weight estimation errors. The effectiveness of the proposed method was validated via numerical simulation of the 2-DOF vehicle lateral dynamics with lateral tire model uncertainties and external disturbances.

Future work includes the extension to all-wheel steering vehicles, practical implementation and validation of the proposed method on a real vehicle, and extension to more complex vehicle models including longitudinal dynamics.

References

[1] H. Tsukamoto, S.-J. Chung, and J.-J. E. Slotine, "Neural stochastic contraction metrics for learning-based control and estimation," *IEEE Control Systems Letters*, vol. 5, no. 5, pp. 1825–1830, 2021.

[2] D. S. Bernstein, *Matrix Mathematics: Theory, Facts, and Formulas (Second Edition)*. Princeton University Press, 2009.

[3] S. Yim, "Comparison among active front, front independent, 4-wheel and 4-wheel independent steering systems for vehicle stability control," *Electronics*, vol. 9, no. 5, 2020.

[4] K. Park, E. Joa, K. Yi, and Y. Yoon, "Rear-wheel steering control for enhanced steady-state and transient vehicle handling characteristics," *IEEE Access*, vol. 8, pp. 149 282–149 300, 2020.

[5] H. Chu, D. Meng, S. Huang, M. Tian, J. Zhang, B. Gao, and H. Chen, "Autonomous high-speed overtaking of intelligent chassis using fast iterative model predictive control," *IEEE Transactions on Transportation Electrification*, vol. 10, no. 1, pp. 1244–1256, 2024.

[6] M. Akar, "Yaw rate and sideslip tracking for 4-wheel steering cars using sliding mode control," in *2006 IEEE Conference on Computer Aided Control System Design, 2006 IEEE International Conference on Control Applications, 2006 IEEE International Symposium on Intelligent Control*, 2006, pp. 1300–1305.

[7] H.-M. Lv, N. Chen, and P. Li, "Multi-objective h ∞ optimal control for four-wheel steering vehicle based on yaw rate tracking," *Proceedings of the Institution of Mechanical Engineers, Part D*, vol. 218, no. 10, pp. 1117–1123, 2004.

[8] T. Eguchi, Y. Sakita, K. Kawagoe, S. Kaneko, K. Mori, and T. Matsumoto, "Development of "super hicas", a new rear wheel steering system with phasereversal control," *SAE Transactions*, vol. 98, pp. 1495–1504, 1989.

[9] W. Lohmiller and J.-J. E. Slotine, "On contraction analysis for non-linear systems," *Automatica*, vol. 34, no. 6, pp. 683–696, 1998.

[10] H. Tsukamoto and S.-J. Chung, "Convex optimization-based controller design for stochastic nonlinear systems using contraction analysis," in *2019 IEEE 58th Conference on Decision and Control (CDC)*, 2019, pp. 8196–8203.

[11] H. Tsukamoto, S.-J. Chung, and J.-J. Slotine, "Learning-based adaptive control using contraction theory," in *2021 60th IEEE Conference on Decision and Control (CDC)*, 2021, pp. 2533–2538.

[12] H. Tsukamoto and S.-J. Chung, "Learning-based robust motion planning with guaranteed stability: A contraction theory approach," *IEEE Robotics and Automation Letters*, vol. 6, no. 4, pp. 6164–6171, 2021.

[13] R. Rajamani, *Vehicle Dynamics and Control*, ser. Mechanical Engineering Series. Springer US, 2011.

[14] B. T. Lopez and J.-J. E. Slotine, "Adaptive nonlinear control with contraction metrics," *IEEE Control Systems Letters*, vol. 5, no. 1, pp. 205–210, 2021.

[15] M. Ryu, J. Kim, and K. Choi, "Imposing a weight norm constraint for neuro-adaptive control," in *2025 European Control Conference (ECC)*, 2025, pp. 380–385.

[16] M. Ryu, N. Monzen, P. Seitter, K. Choi, and C. M. Hackl, "Constrained optimization-based neuro-adaptive control (CONAC) for synchronous machine drives under voltage constraints," in *IECON 2025 – 51st Annual Conference of the IEEE Industrial Electronics Society*, 2025, pp. 1–7.

[17] J. A. Farrell and M. M. Polycarpou, *Adaptive Approximation Based Control: Unifying Neural, Fuzzy and Traditional Adaptive Approximation Approaches (Adaptive and Learning Systems for Signal Processing, Communications and Control Series)*. USA: Wiley-Interscience, 2006.

[18] G. Cybenko, "Approximation by superpositions of a sigmoidal function," *Mathematics of Control, Signals, and Systems (MCSS)*, vol. 2, no. 4, pp. 303–314, Dec. 1989.

[19] H. Tsukamoto, S.-J. Chung, and J.-J. E. Slotine, "Contraction theory for nonlinear stability analysis and learning-based control: A tutorial overview," *Annual Reviews in Control*, vol. 52, pp. 135–169, 2021.

[20] D. Kirk, *Optimal Control Theory: An Introduction*, ser. Dover Books on Electrical Engineering Series. Dover Publications, 2004.

[21] H. Tsukamoto and S.-J. Chung, "Neural contraction metrics for robust estimation and control: A convex optimization approach," *IEEE Control Systems Letters*, vol. 5, no. 1, pp. 211–216, 2021.